

Triangulation

Richard I. Hartley¹ and Peter Sturm²

¹ GE-CRD, Rm K1-5C39, P.O. Box 8, Schenectady NY 12301, USA
Phone: (518)-387-7333, Fax: (518)-387-6845, email: hartley@crd.ge.com

² Lifia-Inria, 46, Avenue Félix Viallet, 38031 Grenoble, France
Phone: (33) 76.57.43.28, Fax: (33) 76.57.46.02, email: Peter.Sturm@lifia.imag.fr

Abstract. In this paper, we consider the problem of finding the position of a point in space given its position in two images taken with cameras with known calibration and pose. This process requires the intersection of two known rays in space, and is commonly known as triangulation. In the absence of noise, this problem is trivial. When noise is present, the two rays will not generally meet, in which case it is necessary to find the best point of intersection. This problem is especially critical in affine and projective reconstruction in which there is no meaningful metric information about the object space. It is desirable to find a triangulation method that is invariant to projective transformations of space. This paper solves that problem by assuming a gaussian noise model for perturbation of the image coordinates. The triangulation problem then may be formulated as a least-squares minimization problem. In this paper a non-iterative solution is given that finds a global minimum. It is shown that in certain configurations, local minima occur, which are avoided by the new method. Extensive comparisons of the new method with several other methods show that it consistently gives superior results.

1 The Triangulation Problem

We suppose that a point \mathbf{x} in R^3 is visible in two images. The two camera matrices P and P' corresponding to the two images are supposed known. Let \mathbf{u} and \mathbf{u}' be projections of the point \mathbf{x} in the two images. From this data, the two rays in space corresponding to the two image points may easily be computed. The triangulation problem is to find the intersection of the two lines in space. At first sight this is a trivial problem, since intersecting two lines in space does not present significant difficulties. Unfortunately, in the presence of noise these rays can not be guaranteed to cross, and we need to find the best solution under some assumed noise model.

A commonly suggested method ([2]) is to choose the mid-point of the common perpendicular to the two rays (the *mid-point method*). Perhaps a better choice would be to divide the common perpendicular in proportion to the distance from the two camera centres, since this would more closely equalize the angular error. Nevertheless, this method will not give optimal results, because of various approximations (for instance the angles will not be precisely equal in the two cases). In the case of projective reconstruction, or affine reconstruction however, the camera matrices, will be known in a projective frame of reference, in which concepts such as common perpendicular, or mid-point (in the projective case) have no sense. In this case, the simple mid-point method here will not work.

The importance of a good method for triangulation is clearly shown by Beardsley et. al. who demonstrate that the mid-point method gives bad results. In [2, 3] they suggest an alternative method based on “quasi-Euclidean” reconstruction. In this method, an approximation to the correct Euclidean frame is selected and the mid-point method is carried out in this frame. The disadvantage of this method is that an approximate calibration of the camera is needed. It is also clearly sub-optimal.

In this paper a new algorithm is described that gives an optimal global solution to the triangulation problem, equally valid in both the affine and projective reconstruction cases. The solution relies on the concepts of epipolar correspondence and the fundamental matrix ([4]). The algorithm is non-iterative and simple in concept, relying on techniques of elementary calculus to minimize the chosen cost function. It is also moderate in computation requirements. In a series of experiments, the algorithm is extensively tested against many other methods of triangulation, and found to give consistent superior performance. No knowledge of camera calibration is needed.

The triangulation problem is a small cog in the machinery of computer vision, but in many applications of scene reconstruction it is a critical one, on which ultimate accuracy depends ([2]).

2 Transformational Invariance

In the last few years, there has been considerable interest in the subject of affine or projective reconstruction ([4, 5, 9, 11, 15, 12, 14]). In such reconstruction methods, a 3D scene is to be reconstructed up to an unknown transformation from the given class. Normally, in such a situation, instead of knowing the correct pair of camera matrices P and P' , one has a pair PH^{-1} and $P'H^{-1}$ where H is an unknown transformation.

A desirable feature of a method of triangulation used is that it should be invariant under transformations of the appropriate class. Thus, denote by τ a triangulation method used to compute a 3D space point \mathbf{x} from a point correspondence $\mathbf{u} \leftrightarrow \mathbf{u}'$ and a pair of camera matrices P and P' . We write

$$\mathbf{x} = \tau(\mathbf{u}, \mathbf{u}', P, P')$$

The triangulation is said to be invariant under a transformation H if

$$\tau(\mathbf{u}, \mathbf{u}', P, P') = H^{-1}\tau(\mathbf{u}, \mathbf{u}', PH^{-1}, P'H^{-1})$$

This means that triangulation using the transformed cameras results in the transformed point. If the camera matrices are known only up to an affine (or projective) transformation, then it is clearly desirable to use an affine (resp. projective) invariant triangulation method to compute the 3D space points.

3 The Minimization Criterion

We assume that the camera matrices, and hence the fundamental matrix, are known exactly, or at least with great accuracy compared with a pair of matching points in the two images. A formula is given in [6] for computing the fundamental matrix given a pair of camera matrices. The two rays corresponding to a matching pair of points $\mathbf{u} \leftrightarrow \mathbf{u}'$ will meet in space if and only if the points satisfy the familiar ([10]) relationship

$$\mathbf{u}'^T F \mathbf{u} = 0 \quad . \quad (1)$$

It is clear, particularly for projective reconstruction, that it is inappropriate to minimize errors in the 3D projective space, \mathcal{P}^3 . For instance, the method that finds the midpoint of the common perpendicular to the two rays in space is not suitable for projective reconstruction, since concepts such as distance and perpendicularity are not valid in the context of projective geometry. In fact, in projective reconstruction, this method will give different results depending on which particular projective reconstruction is considered – the method is not projective-invariant.

Normally, errors occur not in placement of a feature in space, but in its location in the two images, due to digitization errors, or the exact identification of a feature in the image. It is common to assume that features in the images are subject to Gaussian noise which displaces the feature from its correct location in the image. We assume that noise model in this paper.

A typical observation consists of a noisy point correspondence $\mathbf{u} \leftrightarrow \mathbf{u}'$ which does not in general satisfy the epipolar constraint (1). In reality, the correct values of the corresponding image points should be points $\hat{\mathbf{u}} \leftrightarrow \hat{\mathbf{u}}'$ lying close to the measured points $\mathbf{u} \leftrightarrow \mathbf{u}'$ and satisfying the equation $\hat{\mathbf{u}}'^T F \hat{\mathbf{u}}$ exactly. We seek the points $\hat{\mathbf{u}}$ and $\hat{\mathbf{u}}'$ that minimize the function

$$d(\mathbf{u}, \hat{\mathbf{u}})^2 + d(\mathbf{u}', \hat{\mathbf{u}}')^2 \quad , \quad (2)$$

where $d(*, *)$ represents Euclidean distance, subject to the epipolar constraint

$$\hat{\mathbf{u}}'^T F \hat{\mathbf{u}} = 0 \quad .$$

Assuming a Gaussian error distribution, the points $\hat{\mathbf{u}}'$ and $\hat{\mathbf{u}}$ are the most likely values for true image point correspondences. Once $\hat{\mathbf{u}}'$ and $\hat{\mathbf{u}}$ are found, the point \mathbf{x} may be found by any triangulation method, since the corresponding rays will meet precisely in space.

4 An Optimal Method of Triangulation.

In this section, we describe a method of triangulation that finds the global minimum of the cost function (2) using a non-iterative algorithm. If the gaussian noise model can be assumed to be correct, this triangulation method is then provably optimal. This new method will be referred to as the **Polynomial** method, since it requires the solution of a sixth order polynomial.

4.1 Reformulation of the Minimization Problem

Given a measured correspondence $\mathbf{u} \leftrightarrow \mathbf{u}'$, we seek a pair of points $\hat{\mathbf{u}}'$ and $\hat{\mathbf{u}}$ that minimize the sum of squared distances (2) subject to the epipolar constraint $\hat{\mathbf{u}}'^T F \hat{\mathbf{u}} = 0$.

Any pair of points satisfying the epipolar constraint must lie on a pair of corresponding epipolar lines in the two images. Thus, in particular, the optimum point $\hat{\mathbf{u}}$ lies on an epipolar line $\boldsymbol{\lambda}$ and $\hat{\mathbf{u}}'$ lies on the corresponding epipolar line $\boldsymbol{\lambda}'$. On the other hand, any other pair of points lying on the lines $\boldsymbol{\lambda}'$ and $\boldsymbol{\lambda}$ will also satisfy the epipolar constraint. This is true in particular for the point $\bar{\mathbf{u}}$ on $\boldsymbol{\lambda}$ lying closest to the measured point \mathbf{u} , and the correspondingly defined point $\bar{\mathbf{u}}'$ on $\boldsymbol{\lambda}'$. Of all pairs of points on the lines $\boldsymbol{\lambda}$ and $\boldsymbol{\lambda}'$, the points $\bar{\mathbf{u}}$ and $\bar{\mathbf{u}}'$ minimize the squared distance sum (2). It follows that $\hat{\mathbf{u}}' = \bar{\mathbf{u}}'$ and $\hat{\mathbf{u}} = \bar{\mathbf{u}}$, where $\bar{\mathbf{u}}$ and $\bar{\mathbf{u}}'$ are defined with respect to a pair of matching epipolar lines $\boldsymbol{\lambda}$ and $\boldsymbol{\lambda}'$. Consequently, we may write $d(\mathbf{u}, \hat{\mathbf{u}}) = d(\mathbf{u}, \boldsymbol{\lambda})$, where $d(\mathbf{u}, \boldsymbol{\lambda})$ represents the perpendicular distance from the point \mathbf{u} to the line $\boldsymbol{\lambda}$. A similar expression holds for $d(\mathbf{u}', \hat{\mathbf{u}}')$.

In view of the previous paragraph, we may formulate the minimization problem differently as follows. We seek to minimize

$$d(\mathbf{u}, \boldsymbol{\lambda})^2 + d(\mathbf{u}', \boldsymbol{\lambda}')^2 \quad (3)$$

where $\boldsymbol{\lambda}$ and $\boldsymbol{\lambda}'$ range over all choices of corresponding epipolar lines. The point $\hat{\mathbf{u}}$ is then the closest point on the line $\boldsymbol{\lambda}$ to the point \mathbf{u} and the point $\hat{\mathbf{u}}'$ is similarly defined.

Our strategy for minimizing (3) is as follows

1. Parametrize the pencil of epipolar lines in the first image by a parameter t . Thus an epipolar line in the first image may be written as $\boldsymbol{\lambda}(t)$.
2. Using the fundamental matrix F , compute the corresponding epipolar line $\boldsymbol{\lambda}'(t)$ in the second image.
3. Express the distance function $d(\mathbf{u}, \boldsymbol{\lambda}(t))^2 + d(\mathbf{u}', \boldsymbol{\lambda}'(t))^2$ explicitly as a function of t .
4. Find the value of t that minimizes this function.

In this way, the problem is reduced to that of finding the minimum of a function of a single variable, t . It will be seen that for a suitable parametrization of the pencil of epipolar lines the distance function is a rational polynomial function of t . Using techniques of elementary calculus, the minimization problem reduces to finding the real roots of a polynomial of degree 6.

4.2 Details of Minimization.

If both of the image points correspond with the epipoles, then the point in space lies on the line joining the camera centres. In this case it is impossible to determine the position of the point in space. If only one of the corresponding point lies at an epipole, then we conclude that the point in space must coincide with the other camera centre. Consequently, we assume that neither of the two image points \mathbf{u} and \mathbf{u}' corresponds with an epipole.

In this case, we may simplify the analysis by applying a rigid transformation to each image in order to place both points \mathbf{u} and \mathbf{u}' at the origin, $(0, 0, 1)^T$ in homogeneous coordinates. Furthermore, the epipoles may be placed on the x -axis at points $(1, 0, f)^T$ and $(1, 0, f')^T$ respectively. A value f equal to 0 means that the epipole is at infinity. Applying these two rigid transforms has no effect on the sum-of-squares distance function (2), and hence does not change the minimization problem.

Thus, in future we assume that in homogeneous coordinates, $\mathbf{u} = \mathbf{u}' = (0, 0, 1)^\top$ and that the two epipoles are at points $(1, 0, f)^\top$ and $(1, 0, f')^\top$. In this case, since $F(1, 0, f)^\top = (1, 0, f')F = 0$, the fundamental matrix has a special form

$$F = \begin{pmatrix} ff'd - f'c - f'd & & \\ -fb & a & b \\ -fd & c & d \end{pmatrix} .$$

Consider an epipolar line in the first image passing through the point $(0, t, 1)^\top$ (still in homogeneous coordinates) and the epipole $(1, 0, f)^\top$. We denote this epipolar line by $\boldsymbol{\lambda}(t)$. The vector representing this line is given by the cross product $(0, t, 1) \times (1, 0, f) = (tf, 1, -t)$, so the squared distance from the line to the origin is

$$d(\mathbf{u}, \boldsymbol{\lambda}(t))^2 = \frac{t^2}{1 + (tf)^2} .$$

Using the fundamental matrix to find the corresponding epipolar line in the other image, we see that

$$\boldsymbol{\lambda}'(t) = F(0, t, 1)^\top = (-f'(ct + d), at + b, ct + d)^\top .$$

This is the representation of the line $\boldsymbol{\lambda}'(t)$ as a homogeneous vector. The squared distance of this line from the origin is equal to

$$d(\mathbf{u}', \boldsymbol{\lambda}'(t))^2 = \frac{(ct + d)^2}{(at + b)^2 + f'^2(ct + d)^2} .$$

The total squared distance is therefore given by

$$s(t) = \frac{t^2}{1 + f^2t^2} + \frac{(ct + d)^2}{(at + b)^2 + f'^2(ct + d)^2} . \quad (4)$$

Our task is to find the minimum of this function.

We may find the minimum using techniques of elementary calculus, as follows. We compute the derivative

$$s'(t) = \frac{2t}{(1 + f^2t^2)^2} - \frac{2(ad - bc)(at + b)(ct + d)}{((at + b)^2 + f'^2(ct + d)^2)^2} . \quad (5)$$

Maxima and minima of $s(t)$ will occur when $s'(t) = 0$. Collecting the two terms in $s'(t)$ over a common denominator, and equating the numerator to 0 gives a condition

$$\begin{aligned} g(t) &= t((at + b)^2 + f'^2(ct + d)^2)^2 \\ &\quad - (ad - bc)(1 + f^2t^2)^2(at + b)(ct + d) \\ &= 0 . \end{aligned} \quad (6)$$

The minima and maxima of $s(t)$ will occur at the roots of this polynomial. This is a polynomial of degree 6, which may have up to 6 real roots, corresponding to 3 minima and 3 maxima of the function $s(t)$. The absolute minimum of the function $s(t)$ may be found by finding the roots of $g(t)$ and evaluating the function $s(t)$ given by (4) at each of the real roots. More simply, one checks the value of $s(t)$ at the real part of each root (complex or real) of $g(t)$, which saves the trouble of determining if a root is real or complex. One should also check the asymptotic value of $s(t)$ as $t \rightarrow \infty$ to see if the minimum distance occurs when $t = \infty$, corresponding to an epipolar line $-fu = 1$ in the first image.

4.3 Local Minima

The fact that $g(t)$ in (6) has degree 6 means that $s(t)$ may have as many as three minima. In fact, this is indeed possible, as the following case shows. Setting $f = f' = 1$ and

$$F = \begin{pmatrix} 3 & -4 & -3 \\ -2 & 3 & 2 \\ -3 & 4 & 3 \end{pmatrix}$$

gives a function

$$s(t) = \frac{t^2}{1+t^2} + \frac{(4t+3)^2}{(3t+2)^2 + (4t+3)^2}$$

with graph as shown in the left-hand side of Fig 1³ The three minima are clearly shown.

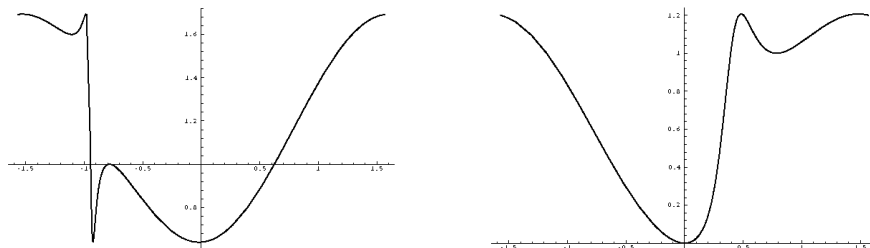


Fig. 1. Left-hand side : *Example of a cost function with three minima. Right-hand side :* *This is the cost function for a perfect point match, which nevertheless has two minima*

As a second example, we consider the case where $f = f' = 1$, and

$$F = \begin{pmatrix} 0 & -1 & 0 \\ 1 & 2 & -1 \\ 0 & 1 & 0 \end{pmatrix} .$$

In this case, the function $s(t)$ is given by

$$s(t) = \frac{t^2}{t^2+1} + \frac{t^2}{t^2+(2t-1)^2}$$

In this case, both terms of the cost function vanish for a value of $t = 0$, which means that the corresponding points \mathbf{u} and \mathbf{u}' exactly satisfy the epipolar constraint. This can be verified by observing that $\mathbf{u}'^T F \mathbf{u} = 0$. Thus the two points are exactly matched. A graph of the cost function $s(t)$ is shown in the right-hand side of Fig 1. One sees apart from the absolute minimum at $t = 0$ there is also a local minimum at $t = 1$. Thus, even in the case of perfect matches local minima may occur. This example shows that an algorithm that attempts to minimize the cost function (2), or equivalently (3) by an iterative search beginning from an arbitrary initial point is in danger of finding a local minimum, even in the case of perfect point matches.

5 Other Triangulation Methods

In this section, we discuss several other triangulation methods that will be compared with the polynomial method.

³ In the graphs in Fig 1 we make the substitution $t = \tan(\theta)$ and plot for θ in the range $-\pi/2 \leq \theta \leq \pi/2$, so as to show the whole infinite range of t .

5.1 Linear Triangulation

The linear triangulation method is the most common one, described for instance in [5]. Suppose $\mathbf{u} = P\mathbf{x}$. We write in homogeneous coordinates $\mathbf{u} = w(u, v, 1)^\top$, where (u, v) are the observed point coordinates and w is an unknown scale factor. Now, denoting by \mathbf{p}_i^\top the i -th row of the matrix P , this equation may be written as follows :

$$wu = \mathbf{p}_1^\top \mathbf{x} \quad , \quad wv = \mathbf{p}_2^\top \mathbf{x} \quad , \quad w = \mathbf{p}_3^\top \mathbf{x} \quad .$$

Eliminating w using the third equation, we arrive at

$$\begin{aligned} u\mathbf{p}_3^\top \mathbf{x} &= \mathbf{p}_1^\top \mathbf{x} \\ v\mathbf{p}_3^\top \mathbf{x} &= \mathbf{p}_2^\top \mathbf{x} \end{aligned} \tag{7}$$

From two views, we obtain a total of 4 linear equations in the coordinates of the \mathbf{x} , which may be written in the form $A\mathbf{x} = \mathbf{0}$ for a suitable 4×4 matrix, A . These equations define \mathbf{x} only up to an indeterminate scale factor, and we seek a non-zero solution for \mathbf{x} . Of course, with noisy data, the equations will not be satisfied precisely, and we seek a best solution.

The Linear-Eigen method. There are many ways to solve for \mathbf{x} to satisfy $A\mathbf{x} = \mathbf{0}$. In one popular method, one finds \mathbf{x} to minimize $\|A\mathbf{x}\|$ subject to the condition $\|\mathbf{x}\| = 1$. The solution is the unit eigenvector corresponding to the smallest eigenvalue of the matrix $A^\top A$. This problem may be solved using the Singular Value Decomposition, or Jacobi's method for finding eigenvalues of symmetric matrices ([13, 1]).

The Linear-LS method. By setting $\mathbf{x} = (x, y, z, 1)^\top$ one reduces the set of homogeneous equations, $A\mathbf{x} = \mathbf{0}$ to a set of 4 non-homogeneous equations in 3 unknowns. One can find a least-squares solution to this problem by the method of pseudo-inverses, or by using the Singular Value Decomposition [13, 1].

Discussion. These two methods are quite similar, but in fact have quite different properties in the presence of noise. The **Linear-LS** method assumes that the solution point \mathbf{x} is not at infinity, for otherwise we could not assume that $\mathbf{x} = (x, y, z, 1)^\top$. This is a disadvantage of this method when we are seeking to carry out a projective reconstruction, when reconstructed points may lie on the plane at infinity. On the other hand, neither of these two linear methods is quite suitable for projective reconstruction, since they are non-projective-invariant. To see this, suppose that camera matrices P and P' are replaced by PH^{-1} and $P'H^{-1}$. One sees that in this case the matrix of equations, A becomes AH^{-1} . A point \mathbf{x} such that $A\mathbf{x} = \epsilon$ for the original problem corresponds to a point $H\mathbf{x}$ satisfying $(AH^{-1})(H\mathbf{x}) = \epsilon$ for the transformed problem. Thus, there is a one-to-one correspondence between points \mathbf{x} and $H\mathbf{x}$ giving the same error. However, neither the condition $\|\mathbf{x}\| = 1$ nor the condition $\mathbf{x} = (x, y, z, 1)^\top$ is invariant under application of the projective transformation H . Thus, in general the point \mathbf{x} solving the original problem will not correspond to a solution $H\mathbf{x}$ for the transformed problem.

For affine transformations, on the other hand, the situation is different. In fact, although the condition $\|\mathbf{x}\| = 1$ is not preserved under affine transformation, the condition $\mathbf{x} = (x, y, z, 1)^\top$ is preserved, since for an affine transformation, $H(x, y, z, 1)^\top = (x', y', z', 1)^\top$. This means that there is a one-to-one correspondence between a vector $\mathbf{x} = (x, y, z, 1)^\top$ such that $A(x, y, z, 1)^\top = \epsilon$ and the vector $H\mathbf{x} = (x', y', z', 1)^\top$ such that $(AH^{-1})(x', y', z', 1)^\top = \epsilon$. The error is the same for corresponding points. Thus, the points that minimize the error $\|\epsilon\|$ correspond as well. Hence, the method **Linear-LS** is affine-invariant, whereas the method **Linear-Eigen** is not. These conclusions are confirmed by the experimental results.

5.2 Iterative Linear Methods.

A cause of inaccuracy in the two methods **Linear-LS** and **Linear-Eigen** is that the value being minimized $\|A\mathbf{x}\|$ has no geometric meaning, and certainly does not correspond to the cost function (2). In addition, multiplying each of the equations (rows of A) by some weight will change the solution. The idea of the iterative linear method is to change the weights of the linear equations adaptively so that the weighted equations correspond to the errors in the image coordinate measurements.

In particular, consider the first of the equations (7). In general, the point \mathbf{x} we find will not satisfy this equation exactly – rather, there will be an error $\epsilon = u\mathbf{p}_3^\top \mathbf{x} - \mathbf{p}_1^\top \mathbf{x}$. What we really want to minimize however, is the difference between the measured image coordinate value u and the projection of \mathbf{x} , which is given by $\mathbf{p}_1^\top \mathbf{x} / \mathbf{p}_3^\top \mathbf{x}$. Specifically, we wish to minimize $\epsilon' = \epsilon / \mathbf{p}_3^\top \mathbf{x} = u - \mathbf{p}_1^\top \mathbf{x} / \mathbf{p}_3^\top \mathbf{x}$. This means that if the equation had been weighted by the factor $1/w$ where $w = \mathbf{p}_3^\top \mathbf{x}$, then the resulting error would have been precisely what we wanted to minimize. The same weight $1/w$ is the correct one to apply to the second equation of (7). For a second image, the correct weight would be $1/w'$ where $w' = \mathbf{p}'_3^\top \mathbf{x}$. Of course, we can not weight the equations in this manner because the weights depend on the value of \mathbf{x} which we do not know until after we have solved the equations. Therefore, we proceed iteratively to adapt the weights. We begin by setting $w_0 = w'_0 = 1$, and we solve the system of equations to find a solution \mathbf{x}_0 . This is precisely the solution found by the linear method **Linear-Eigen** or **Linear-LS**, whichever is being used. Having found \mathbf{x}_0 we may compute the weights.

We repeat this process several times, at the i -th step multiplying the equations (7) for the first view by $1/w_i$ where $w_i = \mathbf{p}_3^\top \mathbf{x}_{i-1}$ and the equations for the second view by $1/w'_i$ where $w'_i = \mathbf{p}'_3^\top \mathbf{x}_{i-1}$ using the solution \mathbf{x}_{i-1} found in the previous iteration. Within a few iterations this process will converge (one hopes) in which case we will have $\mathbf{x}_i = \mathbf{x}_{i-1}$ and so $w_i = \mathbf{p}_3^\top \mathbf{x}_i$. The error (for the first equation of (7) for example) will be $\epsilon_i = u - \mathbf{p}_1^\top \mathbf{x}_i / \mathbf{p}_3^\top \mathbf{x}_i$ which is precisely the error in image measurements as in (2).

This method may be applied to either the **Linear-Eigen** or **Linear-LS** method. The corresponding methods will be called **Iterative-Eigen** and **Iterative-LS** respectively. The advantage of this method over other iterative least-squares minimization methods such as a Levenberg-Marquardt (**LM**) iteration ([13]) is that it is very simple to program. In fact, they require only a trivial adaptation to the linear methods. There is no need for any separate initialization method, as is often required by **LM**. Furthermore the decision on when to stop iterating (convergence) is simple. One stops when the change in the weights is small. Exactly when to stop is not critical, since the change in the reconstructed points \mathbf{x} is not very sensitive to small changes in the weights. The disadvantage of this method is that it sometimes fails to converge. In unstable situations, such as when the points are near the epipoles, this occurs sufficiently often to be a problem (perhaps for 5% of the time). If this method is to be used in such unstable circumstances, then a fall-back method is necessary. In the experiments, we have used the optimal **Polynomial** method as a backup in case convergence has not occurred within 10 iterations. In this way the statistics are not negatively biased by occasional very bad results, due to non-convergence.

Despite the similarities of the properties of the **Iterative-LS** method with an direct non-linear least squares minimization of the goal function 2, it is not identical. Because the **Iterative-LS** method separates the two steps of computing \mathbf{x} and the weights w and w' , the result is slightly different. In fact the three methods **Iterative-LS**, **Iterative-Eigen** and **LM** are distinct. In particular, the methods **Iterative-LS** and **Iterative-Eigen** are not projective-invariant, though experiments show that they are quite insensitive to projective transformation. Of course, **Iterative-LS** is affine-invariant, just as **Linear-LS** is.

Experiments show that the iterative methods **Iterative-LS** and **Iterative-Eigen** perform substantially better than the corresponding non-iterative linear methods.

5.3 Mid-point method

A commonly suggested method for triangulation is to find the mid-point of the common perpendicular to the two rays corresponding to the matched points. This method is relatively easily to compute using a linear algorithm. However, ease of computation is almost its only virtue. This method is neither affine nor projective invariant, since concepts such as perpendicular or mid-point are not affine concepts. It is seen to behave very poorly indeed under projective and affine transformation, and is by far the worst of the methods considered here in this regard.

5.4 Minimizing the sum of the magnitudes of distances

Instead of minimizing the square sum of image errors, it is possible to adapt the polynomial method to minimize the sum of absolute values of the distances, instead of the squares of distances. This method will be called **Poly-Abs**.

The quantity to be minimized is $d(u, \lambda) + d(u', \lambda')$ which, as a function of t , is expressed by

$$s_2(t) = \frac{|t|}{\sqrt{1 + f^2 t^2}} + \frac{|ct + d|}{\sqrt{(at + b)^2 + f'^2 (ct + d)^2}}.$$

Development of this equation leads to a polynomial of degree 8 in t . We evaluate $s_2(t)$ at the roots of this polynomial to find the global minimum of $s_2(t)$.

6 Experimental Evaluation of Triangulation Methods

A large number of experiments were carried out to evaluate the different methods described above. We concentrated on two configurations.

Configuration 1 The first configuration was meant to simulate a situation similar to a robot moving down a corridor, looking straight ahead. This configuration is shown in the left part of Fig 2. In this case, the two epipoles are close to the centre of the images. For points lying on the line joining the camera centres depth can not be determined, and for points close to this line, reconstruction becomes difficult. Simulated experiments were carried out for points at several distances in front of the front camera.

Numerical values we used are as follows:

- The distance between the two cameras is 1 unit.
- The radius of the sphere of observed points is 0.05 units.
- The distance between the center of the point sphere and the projection center of the second camera is chosen as 0.15 or 0.55 units. The center of the sphere lies on the baseline of the two cameras.
- The cameras have the same calibration matrix

$$K = \begin{pmatrix} 700 & 0 & 0 \\ 0 & 700 & 0 \\ 0 & 0 & 1 \end{pmatrix}$$

Configuration 2 In the other configuration, the pair of cameras were almost parallel, as in an aerial imaging situation. The points were assumed to be approximately equidistant from both cameras, with several different distances being tried. This configuration is shown in the right-hand part of figure 2. This was a fairly benign configuration for which most of the methods worked relatively well.

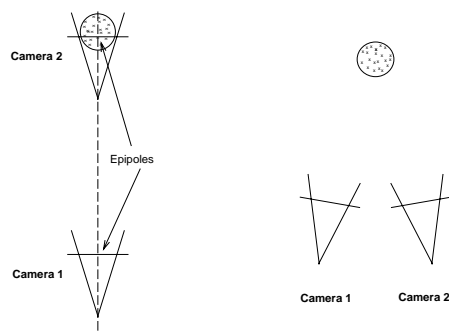


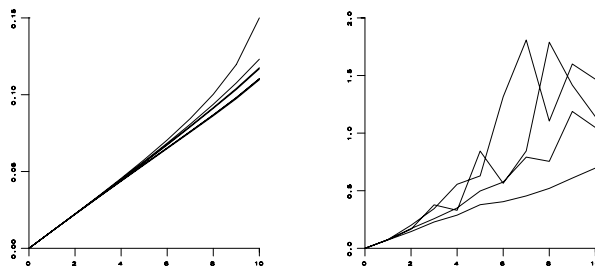
Fig. 2. *The two simulation configurations.*

In each set of experiments, 50 points were chosen at random in the common field of view. For each of several noise levels varying from 1 to 10 pixels (in a 700×700 image), each point was reconstructed 100 times, with different instances of noise chosen from a gaussian random variable with the given standard deviation

(noise level). For each reconstructed point both the 3D reconstruction error, and the 2D residual error (after reprojection of the point) were measured. The errors shown are the average errors. Median errors were also computed. In this latter case the graphs (not shown in this paper) had the same general form and led to the same conclusions. However, they were a little smoother than the graphs shown here, being less sensitive to the occasional gross error.

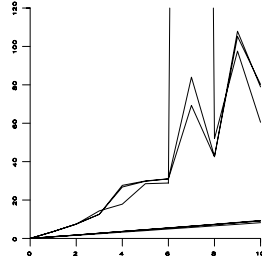
To measure the invariance to transformation, an affine or projective transformation was applied to each camera matrix. The projective and affine transformations were chosen so that one of the camera matrices was of the form $(I \mid 0)$. This is the normalized form of a camera matrix used in the projective reconstruction method of [5]. It represents a significant distortion, since the actual camera matrix was (by construction) of the form $(M \mid 0)$, where M was a diagonal matrix $\text{diag}(700, 700, 1)$.

The most unstable situation is Configuration 1, in which the epipoles are in the centre of the two images, and points lie close to the epipoles. Since this situation gave the most severe test to the algorithms, we will give the results for that configuration. Results of two cases are presented. In one case the points are at a distance of 0.15 units in front of the second camera (near points case) and in the other case, they are at 0.55 units distance (far points case). The results will be presented in the form of graphs with a commentary for each graph. The measured error is denoted either as 2D error (meaning error of measured compared with the reprojected points), or 3D error, meaning the error compared with the correct values of the points in space. In addition, we talk of euclidean, affine and projective reconstruction errors. For affine or projective reconstruction, the camera matrices were transformed by a transformation of the given sort, the triangulation was carried out, and finally the reconstructed points were retransformed into the original frame to compare with the correct values. For euclidean reconstruction, no transformation was carried out. Every data point in the graph is the result of 5000 trials, and expresses the RMS or mean value over all the trials. The horizontal axis of each graph is the noise level (between 0 and 10 pixels RMS in each axial direction), and the vertical axis measures the error, in pixels for 2D error, or in space units for 3D error.

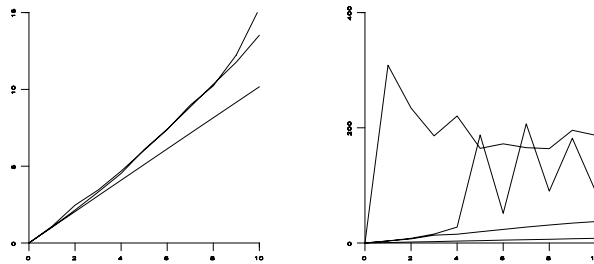


Graph 1 : 3D error for Euclidean reconstruction (near points). *This graph shows all methods. All perform almost equally. Marginally the best results are given by Mid-point, Linear-LS and Iterative-LS, which are almost indistinguishable. The Polynomial method performs marginally worse than the others. It is designed to minimize 2D error, which explains why optimal in this regard, it is not quite optimal for 3D errors. Euclidean reconstruction is the only instance in which Mid-point performed even marginally well, and the only case in which Polynomial and Poly-Abs were beaten.*

Graph 2 : 3D error for Euclidean reconstruction (far points). *The configuration is the same as for Graph 1 except that the points are further from both cameras. The curves from the bottom are Linear-LS, Poly-Abs and then Polynomial and Linear-Eigen which cross each other. The curves for Mid-point and Iterative-LS are identical with Linear-LS, and only one curve is shown. The same is true of Linear-Eigen and Iterative-Eigen.*

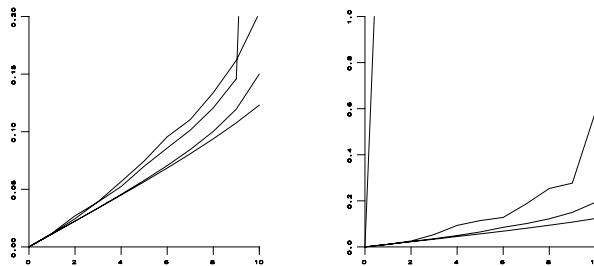


Graph 3 : **2D error for Euclidean reconstruction (near points)** *The configuration is the same as for Graph 1 , except that the average (not RMS) 2D error is measured. Of course Poly-Abs performs best (since it is optimized for this task) but Polynomial, Iterative-LS and Iterative-Eigen are almost indistinguishable. The three very bad performers are Linear-Eigen, Linear-LS and Mid-Point. The maximum Y-scale is 120 pixels. This graph shows that 2D error and 3D error are not well correlated, since despite large 2D errors, these methods perform well in terms of 3D error.*



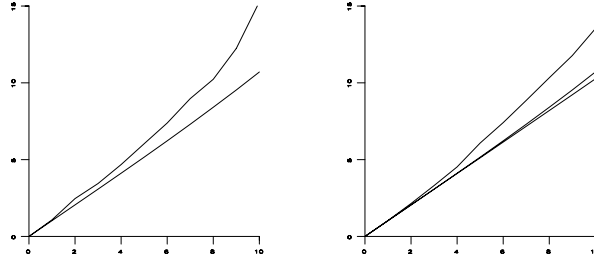
Graph 4 : **2D error for Projective reconstruction (near points)**. *This is the case for which all methods performed well in the Euclidean case. This graph shows the results for methods (from the bottom) Polynomial, Iterative-Eigen, and Iterative-LS. The method Poly-Abs (not shown) performed almost identically with Polynomial. This graph shows that Polynomial, or Poly-Abs is the best method for projective reconstruction, whereas Iterative-Eigen and Iterative-LS (except for occasional non-convergence) perform almost as well. Full Y-scale is 20 pixels.*

Graph 5 : **2D error for Projective reconstruction (near points), continued.** *This shows the average (not RMS) error, to mitigate the effect of outliers. The graphs shown are (from the bottom), Poly-Abs, Linear-Eigen, Linear-LS and Mid-point. Full Y-scale is 400 pixels. This shows how serious a problem non-invariance under transforms can be.*



Graph 6 : **3D error for Projective reconstruction (near points)**. *This is the same as Graph 4 except that we show the 3D error. Poly-Abs performs marginally better than Polynomial. Then follow Iterative-Eigen (except that it fails for noise level of 10 pixels) and Iterative-LS. Full Y-scale is 0.5 units.*

Graph 7 : **3D error for Projective reconstruction (near points), continued.** *The same as Graph 6 for the less well performing methods. From the bottom, are shown Poly-Abs (for reference), Linear-Eigen, Linear-LS and Mid-point (going off scale for noise of 1 pixel). Full Y-scale is 1.0 units.*



Graph 8 : **Comparison of Euclidean (lower curve) and Projective 2D errors.** *The method shown is Iterative-Eigen. The graph shows that this method is almost projective invariant (that is the two curves are almost the same). This would be an excellent method, except for its failure to converge in very unstable situations (about 1% of trials with noise above 2 pixels). The non-converging cases are ignored in this graph. In cases where the points are not near the epipoles non-convergence is not a problem. The method Iterative-LS (not shown) performs similarly, but just slightly worse, whereas Polynomial is exactly projective-invariant (the two curves are superimposed).*

Graph 9 : **Affine Invariance.** *The three curves shown are from the bottom Iterative-Eigen (Euclidean) Iterative-LS (Euclidean and Affine superimposed) and Iterative-Eigen (Affine). Thus, as predicted by theory, the Iterative-LS method is precisely affine-invariant, but Iterative-Eigen is not (but almost). Once more we remark that except for occasional non-convergence, these would be good methods.*

7 Evaluation with real images.

The algorithms were also carried out with the pair of real images shown in Figures 3. These images were the images used for one set of experiments in [2].

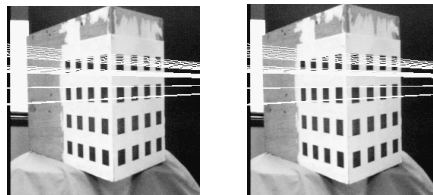
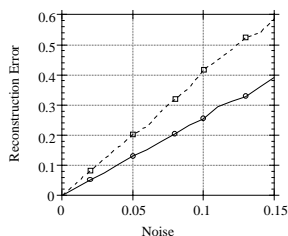


Fig. 3. *Pair of images used for reconstruction experiments, showing matching epipolar lines.*

The goal of these experiments was to determine how the triangulation method effects the accuracy of reconstruction. Since it makes sense to measure the accuracy of reconstruction in a Euclidean frame where distance has a meaning, a close approximation to a correct Euclidean model for the object was estimated by eye and refined using the measured image locations of the corners of the dark squares. The Euclidean model so obtained was used as ground truth.

We desired to measure how the accuracy of the reconstruction varies with noise. For this reason, the measured pixel locations were corrected to correspond exactly to the Euclidean model. This involved correcting each point coordinate by an average of 0.02 pixels. The correction was so small, because of the very great accuracy of the provided matched points. At this stage we had a model and a set of matched points corresponding exactly to the model. Next, a projective reconstruction of the points was computed by the method of [5, 8], and a projective transform H was computed that brought the projective reconstruction into agreement with the Euclidean model. Next, controlled zero-mean Gaussian noise was introduced into the point coordinates, triangulation was carried out in the projective frame, the transformation H was applied, and the error was measured in the Euclidean frame. Graph 10 shows the results of this experiment for two triangulation methods. It clearly shows that the optimal method gives superior reconstruction results.

Note that for these experiments, the projective frame was computed only once, with noiseless data, but triangulation was carried out for data with added noise. This was done to separate the effect of noise on the computation of the projective frame from the effect of noise in the triangulation process. The graph shows the average reconstruction error over all points in 10 separate runs at each chosen noise level.



Graph 10 : Reconstruction Error This graph shows the reconstruction error for the *Mid-point* (above) and *Polynomial* methods. On the horizontal axis is the noise, on the vertical axis the reconstruction error. The units for reconstruction error are relative to a unit distance equal to the side of one of the dark squares in the image. The methods *Linear-LS*, *Linear-Eigen*, *Iterative-LS* and *Iterative-Eigen* gave results close to the *Polynomial* method. Even for the best method the error is large for higher noise levels, because there is little movement between the images. However, for the actual coordinate error in the original matched points (about 0.02 pixels), the error is small.

In this pair of images, the two epipoles are distant from the image. For cases where the epipoles are close to the images, the results on synthetic images show that the advantage of the *Polynomial* methods will be more pronounced.

8 Discussion of Results

All the methods performed relatively for Euclidean reconstruction, as measured in terms of 3D error. In the case of 2D error, only the methods *Polynomial*, *Poly-Abs*, *Iterative-LS* and *Iterative-Eigen* perform acceptably, and the last two have the disadvantage of occasional non-convergence. The **Poly-Abs** method seems to give slightly better 3D error performance than **Polynomial** but both of these seem to be excellent methods, not susceptible to serious failure and giving the best overall 3D and 2D error performance. The only distinct disadvantage is that they are not especially easily generalizable to more than two images. They are a bit slower than the other methods, but by a factor of 2 or 3 only, which is probably not significant.

The **Iterative-LS** method is a good method, apart from the problem of occasional non-convergence. Its advantage is that it is about 3 times as fast as the polynomial method and is nearly projective-invariant. In general **Iterative-LS** seems to perform better than **Iterative-Eigen**, but not very significantly. The big problem, however, is non-convergence. This occurs frequently enough in unstable situations to be a definite problem. If this method is used, there must be a back-up method, such as the polynomial method to use in case of non-convergence.

We summarize the conclusions for the various methods.

Poly This is the method of choice when there are only two images and time is not an issue. It is clearly superior to all other methods, except perhaps **Poly-Abs**. In fact, it is optimum under the assumption of a gaussian noise model. It is affine and projective-invariant.

Poly-Abs This is guaranteed to find the global minimum of sum of magnitude of image error. This may be a better model for image noise, placing less emphasis on larger errors. It seems to give slightly better 3D error results. Otherwise it does not behave much differently from **Poly** and it is affine and projective-invariant.

Mid-point This is not a method that one could recommend in any circumstances. Even for Euclidean reconstruction it is no better than other linear methods, such as *Linear-LS*, which beats it in most other respects. It is neither affine nor projective invariant.

Linear-Eigen The main advantage is speed and simplicity. It is neither affine nor projective invariant.

Linear-LS This has the advantage of being affine invariant, but should not be used for projective reconstruction.

Iterative-Eigen This method gives very good results, markedly better than **Linear-Eigen**, but not quite as good as **Poly**. It may easily be generalized to several images, and is almost projective invariant. The big disadvantage is occasional non-convergence, which occurs often enough to be a problem. It must be used with a back-up method in case of non-convergence.

Iterative-LS This method is similar in performance and properties to **Linear-Eigen**, but should not be used for projective reconstruction, since it does not handle points at infinity well. On the other hand it is affine-invariant.

In summary, the **Polynomial** or **Poly-Abs** method is the method of choice for almost all applications. The **Poly-Abs** method seems to give slightly better 3D reconstruction results. Both these methods are stable, provably optimal, and relatively easy to code. For Euclidean reconstruction, the linear methods are a possible alternative choice, as long as 2D error is not important. However, for affine or projective reconstruction situations, they may be orders of magnitude inferior.

Acknowledgement

Thanks to Paul Beardsley and Andrew Zisserman for making the calibration images and data available to us.

References

1. Atkinson, K.E.: An Introduction to Numerical Analysis, 2nd Edition. John Wiley and Sons, New York (1989).
2. Beardsley, P.A., Zisserman, A., Murray, D.W.: Navigation using affine structure from motion. In Computer Vision - ECCV '94, Volume II, LNCS-Series Vol. 801, Springer-Verlag, 85–96 (1994).
3. Beardsley, P.A., Zisserman, A., Murray, D.W.: Sequential updating of projective and affine structure from motion. Report, Oxford University (1994).
4. Faugeras, O.D.: What can be seen in three dimensions with an uncalibrated stereo rig ? In Computer Vision - ECCV '92, Volume II, LNCS-Series Vol. 588, Springer-Verlag, 563–578 (1992).
5. Hartley, R., Gupta, R., Chang, T.: Stereo from uncalibrated cameras. In Proc. IEEE Conf. on Computer Vision and Pattern Recognition, 761–764 (1992).
6. Hartley, R.I.: Estimation of relative camera positions for uncalibrated cameras. In Computer Vision - ECCV '92, Volume II, LNCS-Series Vol. 588, Springer-Verlag, 579–587 (1992).
7. Hartley, R.I.: Lines and points in three views - an integrated approach. In Proc. ARPA Image Understanding Workshop (1994)
8. Hartley, R.I.: Euclidean reconstruction from uncalibrated views. In Applications of Invariance in Computer Vision, LNCS-Series Vol. 825, Springer-Verlag, 237–256 (1994).
9. Koenderink, J.J., van Doorn, A.J.: Affine structure from motion. Journal of the Optical Society of America, A (1992).
10. Longuet-Higgins, H.C.: A computer algorithm for reconstructing a scene from two projections. Nature, 293, 133–135 (1981).
11. Mohr, R., Veillon, F., Quan, L.: Relative 3d reconstruction using multiple uncalibrated images. In Proc. IEEE Conf. on Computer Vision and Pattern Recognition, 543–548 (1993).
12. Ponce, J., Marimont, D.H., Cass, T.A.: Analytical methods for uncalibrated stereo and motion reconstruction. In Computer Vision - ECCV '94, Volume I, LNCS-Series Vol. 800, Springer-Verlag, 463–470 (1994).
13. Press, W.H., Flannery, B.P., Teukolsky, S.A., Vetterling, W.T.: Numerical Recipes in C: The Art of Scientific Computing. Cambridge University Press (1988).
14. Shapiro, L.S., Zisserman, A., Brady, M.: Motion from point matches using affine epipolar geometry. In Computer Vision - ECCV '94, Volume II, LNCS-Series Vol. 801, Springer-Verlag, 73–84 (1994).
15. Shashua A.: Projective depth: A geometric invariant for 3d reconstruction from two perspective/orthographic views and for visual recognition. In Proc. International Conference on Computer Vision, 583–590 (1993).

This article was processed using the \LaTeX macro package with LLNCS style